ChemComm

COMMUNICATION

View Article Online
View Journal | View Issue

Cite this: *Chem. Commun.*, 2023, 59, 1457

Received 20th December 2022,
Accepted 9th January 2023

DOI: 10.1039/d2cc06908c

rsc.li/chemcomm

Polymerization boosting cascade energy transfer based on opened glucopyranosyl β-cyclodextrin†

Jie Yu,[a] Hui Wang,[a] Xian-Yin Dai,[a] Jie Niu[a] and Yu Liu *[ab]

An injectable polysaccharide supramolecular hydrogel was successfully fabricated from opened D-glucopyranosyl β-cyclodextrin with four aldehyde groups (ACD) cross-linked with biomacromolecule chitosan (CS), which was not only beneficial to the clustering-triggered emission of CS with high quantum yield (32.25%), but also could co-assemble with a first stage acceptor triphenylamine derivative (TPA) and encapsulate Cyanine 5 (Cy5) or Nile blue (NiB) achieving supramolecular cascade energy transfer from the cross-linked polymer to the dyes, leading to fluorescence emission at 673 nm or 680 nm, and could be further applied in cell imaging.

Possessing carboxyl, amino, hydroxyl and amide groups, many biomacromolecules can be conveniently modified with functional chromophores and have good solution process-ability as well as biocompatibility, exhibiting wide application prospects in luminescent materials,[1–3] biological imaging,[4] selective detection[5,6] and drug delivery.[7,8] Benefitting from the luminescent properties of biomacromolecules, the biocompatible luminogens display unique luminescent properties different from traditional conjugated or aromatic luminophores. For example, Tang and Yan found that poly-L-lysine could assemble with oleate to form more compact and ordered supramolecular assemblies in the solid phase and gave circularly polarized fluorescence.[9] Yuan *et al.* reported that sodium alginate could crosslink with Ca^{2+} ions, exhibiting luminescence emission in solution and prolonged room temperature phosphorescence in the solid phase, showing wide applications in bioimaging and optoelectronics.[4]

On the other hand, β-cyclodextrins (β-CDs) comprising seven D-glucose units can be used as important building blocks for the construction of luminescence systems due to their low toxicity, good biocompatibility and confined microenvironment for luminophores.[10–13] Recently, Yang *et al.* reported that the two bipyrene-modified γ-cyclodextrin derivatives, in which the pyrene units could interpenetrate into the rigid chiral cavities of the host, achieved circularly polarized luminescence and assembled to form a supramolecular polymer with a fluorescence quantum efficiency up to 64.1%.[14] We reported a long lifetime NIR luminescence system based on the encapsulation of macrocycles and assembly confinement of β-CD modified hyaluronic acid (HACD).[15] Benefitting from the reaction of β-CD and sodium periodate gave the opened glucopyranose units of β-CD with four aldehyde groups randomly substituted (ACD), which should be easy to react with biomacromolecules containing amino groups under acid catalysis to give cross-linked polymers and may provide a platform for the construction of luminescence systems. In particular, the cross-linking of cyclodextrin with biomacromolecules to form a luminescent supramolecular gel as an energy donor and further fabricate a cascade energy transfer system has not been reported, as best we know.

A luminescent injectable polysaccharide supramolecular hydrogel was successfully synthesized by ACD cross-linked with CS *via* Schiff-base reaction, which exhibited strong fluorescence emission at 425 nm with a high quantum yield (32.25%) (Scheme 1). In this system, ACD was not only used as the cross-linking reagent of the hydrogel, but was also beneficial to the formation of regional confined rigid structures in ACD/CS, giving strong blue fluorescence emission. The luminescent cross-linked polymer could load triphenylamine derivatives with zwitterionic groups and a rigid tripaddle core (TPA) through electrostatic interaction to form an injectable supramolecular hydrogel, which exhibited efficient energy transfer from luminescent structures to TPA with an energy transfer efficiency (E) up to 86%. Moreover, tunable multicolor luminescence from blue to yellow was feasibly achieved by the gradient doping of the triphenylamine derivative, including white-light emission. Furthermore, the supramolecular polymer of ACD/CS/TPA could bind with Cy5 or NiB by host–guest interaction, leading to efficient cascade energy transfer from the cross-linked polymer to dye acceptors (E = 68.3% for NiB), giving near-infrared (NIR)

[a] *College of Chemistry, State Key Laboratory of Elemento-Organic Chemistry, Nankai University, Tianjin 300071, P. R. China. E-mail: yuliu@nankai.edu.cn*
[b] *Haihe Laboratory of Sustainable Chemical Transformations, Tianjin 300192, China*

† Electronic supplementary information (ESI) available: Experimental procedures, characterization data, and spectral data. See DOI: https://doi.org/10.1039/d2cc06908c

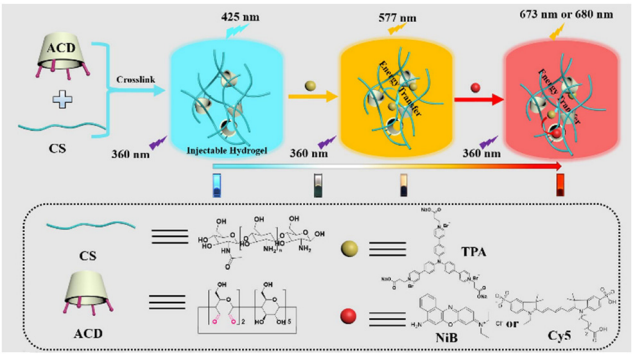

Scheme 1 Polymerization boosting cascade energy transfer based on opened glucopyranosyl β-cyclodextrin.

luminescence at 673 nm or 680 nm, respectively. Finally, the obtained supramolecular polymer with cascade energy transfer performance was successfully applied in NIR cell imaging.

Firstly, the ACD was synthesized by the reaction of β-CD with sodium periodate (Fig. S1, ESI†).[16,17] Under the catalysis of acetic acid, the aldehyde groups of ACD could react with the amino of chitosan to form the units of C═N double bonds, thus leading to a cross-linked polymer (Scheme 1). Considering that the chitosan with a stable hydrophilic structure is beneficial to form a hydrogel, we explored the critical gelation concentration (CGC) of this polysaccharide. The hydrogel was formed when the total concentration of chitosan and ACD was 40 mg mL^{-1}, and the content of gel factor was measured to be 3.8% (Table S1, ESI†). The control experiments showed that neither chitosan nor the simple mixture of β-CD and chitosan could form a hydrogel (Fig. S2, ESI†). Therefore, we preliminarily speculated that ACD could react with chitosan to give the polysaccharide hydrogel. We further characterized the ACD/CS hydrogel by solid-state NMR, X-ray photoelectron spectroscopy (XPS), scanning electron microscopy (SEM) and rheometer analysis experiments. Fig. 1(a) shows that after ACD reacted with chitosan, the NMR signal of the aldehyde group at 199.5 ppm[17] disappeared and a new peak at 179.5 ppm was observed, which was ascribed to the signal of C═N bonds, implying the formation of Schiff-base structures. In the C1S spectrum of ACD/CS, the peak at 287.4 eV was assigned to the characteristic signal of the C═N structure (Fig. S3, ESI†).[16,17] The observed peak at 399.1 eV in the N1S data of ACD/CS further confirmed the formation of Schiff-base units in the hydrogel (Fig. 1(b)). The signals at 404.1 eV and 396.8 eV were assigned to N–H and C–N bonds,[5,6] respectively, manifesting that there still existed unreacted amino groups in the system. In Fig. 1(c), a honeycomb porous-like xerogel was observed in the SEM image, indicating that ACD/CS formed a crosslinked polysaccharide polymer.

The mechanical properties of the hydrogel were also explored by rheometer analysis experiments. The force–strain sweep test (Fig. S4, ESI†) showed that the polymer of ACD/CS kept the structure of the hydrogel in the shear strain range from 0.1 to 100%. Fig. 1(d) exhibits that the storage modulus (G') value of ACD/CS was larger than the loss modulus (G'') at 1% strain, implying that ACD/CS has a stable hydrogel structure.[18] Furthermore, the hydrogel can be stored in a syringe and then injected onto a glass plate to form the numbers "517" (ESI,† Video).

The ACD/CS gel without aromatic groups gave blue luminescence under an ultraviolet lamp (Fig. S5, ESI†), which inspired us to explore the photophysical properties of ACD/CS. In Fig. 2(a), both ACD and CS gave negligible fluorescence signal, in sharp contrast, the ACD/CS exhibited blue luminescence emission at 425 nm. The absorption spectrum clearly showed that the ACD/CS hydrogel gave a peak at 315 nm belonging to the n–π* transition of the C═N bond (Fig. 2(b)). However, the excitation spectrum of ACD/CS was not completely coincided with the ultraviolet band. The signal intensity of ACD/CS at 360 nm was obviously higher than that of ACD or CS (Fig. S6, ESI†), which may be ascribed to ACD/CS with aggregated structures that further enhanced the n–π* transition of the C═N bonds.[5,6,19] The fluorescence emission peak of ACD/CS

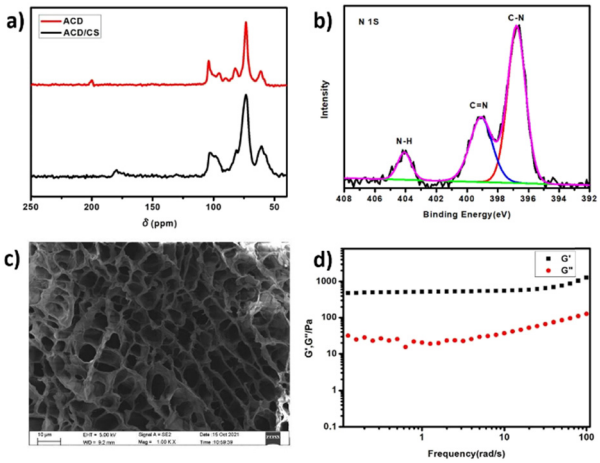

Fig. 1 (a) Solid ^{13}C NMR (100 MHz) spectrum of ACD and ACD/CS. (b) N1s X-ray photoelectron spectrum of ACD/CS. (c) SEM image of ACD/CS. (d) Frequency sweep tests of ACD/CS were performed at 1% strain (G': storage modulus; G'': loss modulus).

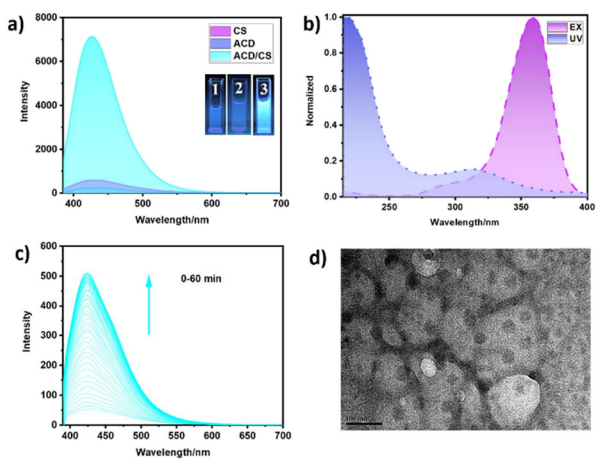

Fig. 2 (a) Fluorescence spectrum of CS, ACD and ACD/CS. Inset: 1: CS, 2: ACD, 3: ACD/CS under 365 nm light. (b) Excitation (EX) and absorption (UV) spectrum of ACD/CS. (c) Fluorescence spectrum of ACD/CS with different heating times at 50 °C. (d) TEM image of ACD/CS.

was red-shifted from 422 nm to 465 nm under different excitation wavelengths (300 nm to 400 nm, Fig. S7, ESI†). This was probably because of the various aggregation patterns of ACD/CS with the multiple space conjugation of C=N bonds to form different luminescence sites.[19,20] Notably, ACD/CS gave weak luminescence in diluted solution (such as 1.6 and 2.4 mg mL^{-1}, Fig. S8, ESI†), but the fluorescence intensity was enhanced with the increase of the concentration of ACD/CS from 5.6 to 40 mg mL^{-1}, exhibiting aggregation-induced emission (AIE) characteristics. From the above experiment results, the clustering-triggered emission (CTE) mechanism could account for the fluorescence emission of ACD/CS. Additionally, the fluorescence signals of ACD/CS at different times showed that the luminescence intensity of the system was increased with the Schiff-base reaction between ACD and CS and reached a stable level after 60 min (Fig. 2(c) and Fig. S9, ESI†), which further confirmed that the luminescence emission was related to the formation of clustered ACD/CS with C=N bonds. More evidence comes from the morphology of ACD/CS. The TEM image showed that many nanoparticles with diameter about 30 nm were formed by the aggregation of ACD/CS (Fig. 2(d)).

Different from the previously reported weak luminescence biomacromolecule systems,[1–6] the ACD/CS exhibited high fluorescence quantum yield (32.25%) (Fig. S10, ESI†), which may be induced by the confinement of ACD. As a crosslinking reagent, possessing a cyclic structure and many hydroxyl groups, ACD could react with chitosan to give C=N double bonds at the outside of the ACDs' cavities, benefiting the clustering of the C=N bonds in ACD/CS. Moreover, the multi-hydroxyl groups in ACD are also favourable to form abundant hydrogen bonds. These merits are beneficial to the conjugation of lone pair electrons in the cluster structures, leading to efficient luminescence.[19,20] Furthermore, the study on the photostability of the hydrogel showed that the fluorescence intensity of ACD/CS had no obvious change after 1 hour irradiation (Fig. S11 and S12, ESI†), indicating that the luminescent hydrogel possess good resistance of photobleaching.

The ACD/CS not only has good photophysical properties but also can be conveniently prepared, which may act as a donor in energy transfer systems. The triphenylamine derivative with zwitterionic groups and a rigid tripaddle core was synthesized and characterized by NMR experiments (Fig. S13 and S14, ESI†), and then was added in the ACD/CS as an energy acceptor. The absorption band of the selected chromophore and the luminescence spectrum of ACD/CS exhibited a good overlap region at 400–500 nm (Fig. 3(a)). Thus, the energy transfer process may occur in this system. On the other hand, anionic carboxylates of TPA could interact with cationic groups of ACD/CS polymer through electrostatic interaction, which also shortens the space distance between the luminogens and the chromophore, thus benefitting energy transfer. When different amounts of TPA were doped into the system (Fig. 3(b)), the luminescence of ACD/CS was gradually quenched and the emission from TPA was raised, accompanied by the luminescence colour of the system changing from blue to yellow, indicating the energy transfer from ACD/CS to TPA. It is noteworthy that upon the addition of TPA (Fig. 3(c)), white light luminescence was observed

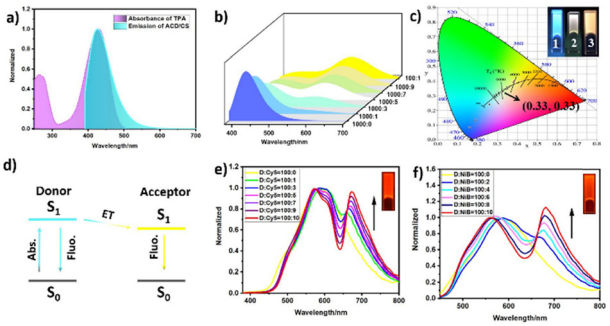

Fig. 3 (a) Normalized UV-vis band of TPA and fluorescence spectrum of ACD/CS. (b) Fluorescence spectrum of ACD/CS in the presence of different amounts of TPA (based on ACD equivalent). (c) CIE diagram of ACD/CS/TPA. Inset: 1: blue (ACD/CS : TPA = 1000 : 0), 2: white (ACD/CS : TPA = 1000 : 5), 3: yellow (ACD/CS : TPA = 100 : 1). (d) Proposed possible energy transfer mechanism. Normalized fluorescence spectrum of ACD/CS/TPA in the presence of different amounts of Cy5 (e) and NiB (f) (D: ACD/CS/TPA).

(ACD/CS : TPA = 1000 : 5), and the CIE diagram gave coordinates of (0.33, 0.33). According to the intensity change of the luminescence at 425 nm (Fig. S15, ESI†), the E of this system was measured to be 86% in the presence of TPA (ACD/CS : TPA = 100 : 1). More control experiments were carried out to further confirm the energy transfer from ACD/CS to TPA. In Fig. S15 (ESI†), both ACD/TPA and CS/TPA gave negligible luminescence signals. In addition, the excitation spectrum of ACD/CS/TPA showed that the signal intensity at 360 nm was obviously enhanced (Fig. S16, ESI†), implying that the fluorescence emission of TPA was ascribed to the energy transfer from excited ACD/CS to TPA. Furthermore, the time-resolved decay traces (Fig. S17, ESI†) manifested that the fluorescence lifetime of ACD/CS at 425 nm was 6.04 ns, and then decreased to 3.36 ns after adding TPA. These results jointly confirmed that the energy transfer from ACD/CS to the chromophore in this supramolecular polymer should be a Förster mechanism.[21] Based on the above results, we proposed a possible energy transfer mechanism in this system. The energy transfer from the singlet state of ACD/CS (donor) to the acceptor, further turns to the ground state and generates the fluorescence of the acceptor (Fig. 3(d)).

The ACD/CS/TPA not only exhibits first-stage highly efficient energy transfer, but also contains cyclodextrin cavities that can bind dyes as an energy acceptor to construct a cascade energy transfer system, realizing NIR fluorescence emission. As shown in Fig. S18 (ESI†), the absorption bands of NIR and Cy5 were overlapped with the emission spectrum of TPA in the wavelength range of 400–700 nm, indicating that the two dyes may act as the second energy acceptors. Subsequently, different amounts of Cy5 or NiB were added into the ACD/CS/TPA, and a NIR signal at 673 nm or 680 nm was observed in Fig. 3(e) and (f), indicating the energy transfer from the excited ACD/CS/TPA to the second-stage acceptors. When the ratio of donor to acceptor was 10 : 1, according to the fluorescence signal change at 577 nm, the second stage energy transfer efficiency was calculated as 51.5% and 68.3% for Cy5 and NiB, respectively (Fig. S19 and S20, ESI†). In addition, the binding constants

between ACD and Cy5 or NiB were calculated as $2.55 \times 10\ M^{-1}$ and $4.83 \times 10\ M^{-1}$ (Fig. S21 and S22, ESI†), respectively, indicating that ACD could effectively encapsulate the selected secondary acceptors. Therefore, the supramolecular polymer of ACD/CS provides a confined microenvironment for the acceptors in the secondary energy transfer system, which is conducive to energy transfer from the luminescent polymer to the acceptors, leading to efficient NIR fluorescence emission. In order to explore the energy transfer mechanism of this system, Cy5 or NiB was also added into the polymer of ACD/CS, but no NIR signal was observed (Fig. S23, ESI†), indicating that the energy could not be directly transferred from excited state ACD/CS to the second stage acceptors. Furthermore, Fig. S24 (ESI†) showed that the fluorescence lifetime of ACD/CS/TPA at 577 nm (2.37 ns) exhibited no obvious change in the presence of NiB (2.29 ns) and Cy5 (2.32 ns), respectively, indicating that the energy transfer from TPA to the acceptors should go through a non-radiative transfer path.[22]

We put the prepared hydrogels in a syringe and loaded it on a glass plate. Then blue ''N'', white ''K'' and yellow ''U'' were observed under the 365 nm (Fig. S25a and b, ESI†). We also coated the ACD/CS/TPA on the surface of the diode with 365 nm light, and then the bright white luminescence could be clearly observed (Fig. S25c and d, ESI†). Considering that the main components of this luminescent hydrogel are chitosan and cyclodextrin derivatives, two kinds of polysaccharides with good biocompatibility, we also explored the possible application of this polysaccharide hydrogel in cell imaging. First, the cytotoxicity of ACD/CS was measured by an *in vitro* cell experiment. The survival rate of normal cells was up to $104 \pm 3.7\%$ at 5 mg mL^{-1} after being treated with ACD/CS for 24 hours (Fig. S26, ESI†), indicating that the obtained hydrogel has good biocompatibility. Subsequently, the supramolecular hydrogel with cascade energy acceptors was also added into A549 cells and incubated for 12 h. As shown in Fig. S27a and c (ESI†), the red fluorescence from the cascade energy transfer system was observed in cancer cells, indicating that this luminescent hydrogel has the ability of cell imaging.

In conclusion, a luminescent injectable polysaccharide supramolecular hydrogel was successfully constructed by ACD cross-linked with chitosan, and exhibited bright blue fluorescence emission benefitting from the rigid structures with C=N groups, mainly occuring through a CTE mechanism. By the gradient doping of TPA in this luminescent polymer, efficient energy transfer from the excited cross-linked polymer to TPA was observed, which was also accompanied by tunable multicolor luminescence from blue to yellow, including white CIE chromaticity coordinates (0.33, 0.33). Furthermore, the co-assembly of ACD/CS/TPA could encapsulate Cy5 or NiB to form a supramolecular cascade energy transfer system with NIR fluorescence emission at 673 nm or 680 nm. Finally, this biocompatible supramolecular hydrogel with energy transfer performance has been successfully applied in NIR cell imaging.

We thank the National Natural Science Foundation of China (22201142 and 22131008) and the Haihe Laboratory of Sustainable Chemical Transformations for financial support.

Conflicts of interest

There are no conflicts to declare.

Notes and references

1 S. Y. Tao, S. J. Zhu, T. L. Feng, C. Y. Zheng and B. Yang, *Angew. Chem., Int. Ed.*, 2020, **59**, 9826–9840.
2 Z. Zhao, H. K. Zhang, J. W. Y. Lam and B. Z. Tang, *Angew. Chem., Int. Ed.*, 2020, **59**, 9888–9907.
3 J. Y. Zhang, L. R. Hu, K. H. Zhang, J. K. Liu, X. G. Li, H. R. Wang, Z. Y. Wang, H. H. Y. Sung, I. D. Williams, Z. B. Zeng, J. W. Y. Lam, H. K. Zhang and B. Z. Tang, *J. Am. Chem. Soc.*, 2021, **143**, 9565–9574.
4 X. Y. Dou, Q. Zhou, X. H. Chen, Y. Q. Tan, X. He, P. Lu, K. Y. Sui, B. Z. Tang, Y.-M. Zhang and W. Z. Yuan, *Biomacromolecules*, 2018, **19**, 2014–2022.
5 (*a*) J. Y. Song, H. J. Zhou, R. Gao, Y. Zhang, H. M. Zhang, Y. X. Zhang, G. Z. Wang, P. K. Wong and H. J. Zhao, *ACS Sens.*, 2018, **3**, 792–798; (*b*) Z. Li and Y.-W. Yang, *Adv. Mater.*, 2022, **34**, 2107401.
6 (*a*) Z. Y. Wang, H. K. Zhang, S. Q. Li, D. Y. Lei, B. Z. Tang and R. Q. Ye, *Top. Curr. Chem.*, 2021, **379**, 14; (*b*) Z. Li, Z. Yang, Y. Zhang, B. Yang and Y.-W. Yang, *Angew. Chem., Int. Ed.*, 2022, **61**, e202206144.
7 J. Yu, Y. Chen, Y.-H. Zhang, X. Xu and Y. Liu, *Org. Lett.*, 2016, **18**, 4542–4545.
8 X.-Y. Dai, B. Zhang, Q. Yu and Y. Liu, *J. Med. Chem.*, 2022, **65**, 7363–7370.
9 P. L. Liao, S. H. Zang, T. Y. Wu, H. J. Jin, W. K. Wang, J. B. Huang, B. Z. Tang and Y. Yan, *Nat. Commun.*, 2021, **12**, 5496.
10 W.-L. Zhou, Y. Chen, W. J. Lin and Y. Liu, *Chem. Commun.*, 2021, **57**, 11443–11456.
11 Z. Z. Dong, Y. Z. Bi, H. R. Cui, Y. D. Wang, C. L. Wang, Y. Li, H. W. Jin and C. Q. Wang, *ACS Appl. Mater. Interfaces*, 2019, **11**, 23840–23847.
12 L. H. Bai, H. X. Yan, T. Bai, Y. B. Feng, Y. Zhao, Y. Ji, W. X. Feng, T. L. Lu and Y. F. Nie, *Biomacromolecules*, 2019, **20**, 4230–4240.
13 W. Y. Li, J. L. Qu, J. W. Du, K. F. Ren, Y. X. Wang, J. Z. Sun and Q. L. Hua, *Chem. Commun.*, 2014, **50**, 9584–9587.
14 C. l Tu, W. H. Wu, W. T. Liang, D. J. Zhang, W. Xu, S. Wan, W. Lu and C. Yang, *Angew. Chem., Int. Ed.*, 2022, **61**, e202203541.
15 X.-Y. Dai, M. Huo, X. Dong, Y.-Y. Hu and Y. Liu, *Adv. Mater.*, 2022, 2203534.
16 Q. J. Li, D. D. Wang, X. Fang, X. Y. Wang, S. Mao and K. K. Ostrikov, *Adv. Funct. Mater.*, 2021, 2104572.
17 Q. J. Li, D. D. Wang, X. Fang, B. Y. Zong, Y. Liu, Z. Li, S. Mao and K. K. Ostrikov, *Chem. Commun.*, 2021, **57**, 1161–1164.
18 J. Niu, Y. Chen and Y. Liu, *Chin. J. Org. Chem.*, 2019, **39**, 151–156.
19 B. Chu, H. K. Zhang, L. F. Hu, B. Liu, C. J. Zhang, X. H. Zhang and B. Z. Tang, *Angew. Chem., Int. Ed.*, 2022, **61**, e202114117.
20 S. Tang, T. J. Yang, Z. H. Zhao, T. W. Zhu, Q. Zhang, W. B. W. Hou and W. Z. Yuan, *Chem. Soc. Rev.*, 2021, **50**, 12616–12655.
21 J. Yu, H. Wang and Y. Liu, *Adv. Opt. Mater.*, 2022, **10**, 2201761.
22 J. Yu, H. Wang, X.-Y. Dai, Y. Chen and Y. Liu, *ACS Appl. Mater. Interfaces*, 2022, **14**, 4417–4422.

